EPJ Web of Conferences **66**, 03038 (2014)
DOI: 10.1051/epjconf/ 20146603038
© Owned by the authors, published by EDP Sciences, 2014

Calculation of vector analyzing power in the p+^{6,8}He elastic scattering at intermediate energies

Elena Ibraeva[1a], Onlasun Imambekov[2]

[1]Institute of Nuclear Physics, 050032, str. Ibragimova 1, Almaty, Kazakhstan
[2]Al-Farabi Kazakh National University, 050040, av. Al-Farabi 71, Almaty, Kazakhstan

Abstract. A calculations of the analyzing power (A_y) of the elastic proton scattering on ^{6}He and ^{8}He are presented in the framework of the Glauber multiple diffraction scattering at E = 71 and 1000 MeV/nucleon. The wave functions obtained in the three-body α-n-n-model for ^{6}He and the density distribution function in the no-core shell model for ^{8}He are used. Our calculations qualitatively reproduced the data of A_y for p^6He and p^8He scattering and compare with the calculations' results in the other approaches.

1 Introduction

The first reliable measurements of the vector analyzing power in elastic p^6He and p^8He-scattering at 71 MeV/nucleon have been made recently at the RIKEN accelerator [1-3]. An appearance of such type of date makes it possible to test different model calculations that take into account the spin-orbit interaction, because the spin-orbit coupling in nuclei manifests itself in the polarization phenomena in nuclear elastic scattering.

The ^{6}He and ^{8}He nuclei are neutron-excess β-radioactive with the dominant $\alpha + 2n$ and $\alpha + 4n$ structure. The facts justifying the α-n-n-model of ^{6}He and the α-2n-2n-model of ^{8}He are the fellowing low binding energies in the channel α-2n ($E_{\alpha\text{-}2n}$ = 0.973 MeV [4]) and α-4n ($E_{\alpha\text{-}4n}$ = 3.1 MeV [4]), spectroscopic factors of α-2n and α-4n channels close to one. Also the measurement of the differential cross sections of high-energy proton scattering on ^{6}He and ^{8}He in inverse kinematics [5-8] shows the evidence of the well-defined clustering of these nuclei on α-partial core and valence nucleons, which form halo or skin with the radius about 0.9 fm. The analysis of the differential cross sections of p^6He and p^8He-scattering carried out in the full microscopic folding-model [9] with wave function in (0+2+4) $\hbar\omega$ model space concluded that ^{6}He is a typical halo nucleus, while ^{8}He has no halo, but can have a neutron skin. The newest analyses of the analyzing power data for the ^{6}He and ^{8}He scattering from hydrogen at E = 71 MeV/nucleon has been presented in [10]. The g-folding approach based on the multi-$\hbar\omega$ no-core shell model wave functions (WFs), agrees with analyzing power data.

We calculated the analyzing power (A_y) of the elastic scattering of protons on the ^{6}He and ^{8}He isotopes made in the framework of the Glauber multiple diffraction scattering at E = 71 and 1000 MeV/nucleon. We use the WFs obtained in the three-body α-n-n-model for ^{6}He [11, 12] and the density distribution function in the large scale shell model for ^{8}He [9]. These are three-body α-n-n

[1] Contact email: ibraeva.elena@gmail.com

This is an Open Access article distributed under the terms of the Creative Commons Attribution License 2.0, which permits unrestricted use, distribution, and reproduction in any medium, provided the original work is properly cited.

functions for ^{6}He calculated by the variational method with different intercluster interaction potentials. The *n*-*n* potential is the same for both models. The *α*-*n* potential is the Sack-Biedenharn-Breit potential in model 1 [11] and the potential split in orbital-angular momentum parity in model 2 [12].

The details of calculation were presented in [13].

2 Results and Discussion

Figure 1 show A_y for p^6He scattering at $E = 71$ MeV/nucleon (a) and $E = 1000$ MeV/nucleon (b). The curves 1, 2 and 3 − our calculation with the WFs in models 1 and 2 and shell model one. The curves 4, 5, 6 are from [2]. The experimental data in Fig. 1a are from [1, 2].

Our calculations (see Figs. 1a and 1b) show that A_y has approximately the same behavior at small angles for all model WFs, despite significant differences of three-body and oscillator WFs of ^{6}He.

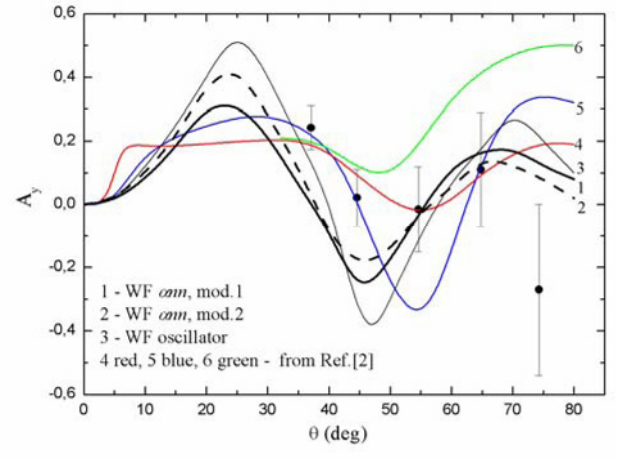

Fig. 1a. The vector analyzing power of p^6He scattering at $E = 71$ MeV/nucleon. Experimental data are from [1, 2]. Explanations are given in the text.

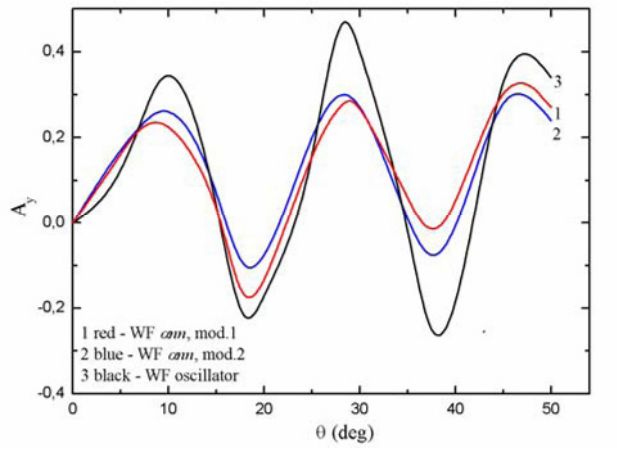

Fig. 1b. The same as in Fig. 1a but at $E = 1000$ MeV/nucleon. Explanations are given in the text.

The fact that the calculated curves have the same behavior at small angles (corresponds to small momentum transfer), suggests a weak influence of the peripheral region of the nucleus (scattering on

neutron skin or halo) on A_y. This is explained by a small contribution of the spin-orbit interaction to the valence neutrons near zero at small momentum transfers.

Increase of the amplitude of A_y with angle increasing (and momentum transfer) indicates of significant sensitivity of the analyzing power to the distribution of nucleons in the central region of the nucleus. Essentially different from each other in oscillations size, all calculated curves reach their maximum and minimum values at the same angles. As the energy increases from 71 to 1000 MeV/nucleon, the number of oscillations increases.

Comparison of our calculations with the data [1,2] in Fig. 1a shows only qualitative agreement; in particular, all the curves change the sign from positive to negative at $\theta \sim 40°$.

For comparison, Fig. 1a shows the results of calculation with this characteristic from [2] (curves 4, 5, 6). The results obtained in [2] were analyzed in the optical model with several potentials: phenomenological, folding (cluster and nucleon) and non-local one in full microscopic model with three sets of single-particle WFs (Woods-Saxon with halo, without halo and with oscillator one). The authors were able to provide a quantitative description of the data only with the phenomenological optical potential with special fitting of the parameters (curve 4). The calculation in the cluster folding-model with increased values r_0 and a is in only qualitative agreement with the experiment (curve 5). Other calculations (curve 6) do not result in satisfactory description of A_y. The example is curve 6, calculated in the microscopic model with the Woods-Saxon WF with the halo.

Figures 2a and 2b show a comparison of A_y for the p^6He (curve 1 is the same as the curve 1 in Figs. 1a and 1b) and for the p^8He (curve 2) scattering at 70 (a) and 1000 (b) MeV/nucleon. Figures show that the analyzing powers for p^6He and p^8He are very similar. However, the mass effect of ^{8}He valence neutrons is that A_y for p^8He is slightly shifted to the region of smaller angles compared to p^6He scattering at both energies. The last calculations of this characteristic were carried out in [10] using distorted wave approximation (DWA). The wave function of ^{8}He specified from a no-core shell model used a complete (0+2+4)~ħω basis. In Fig. 2a we show the curve 3 [10], which is in better agreement with the data in this case. The DWA describes A_y at such low energy more realistically, because there are no energetic or angular limitations, that exist in the Glauber approximation.

Comparison of the analyzing powers of $p^{4,6,8}$He and p^6Li scattering, made in [2], revealed interesting features of their behavior. The vector analyzing powers for p^6He and p^4He have the same behavior (changing the sign from positive to negative at $\theta \sim 60°$), whereas A_y for p^6Li scattering is positive and increases smoothly without changing the sign. As we mentioned above it was much more complicated to reproduce the analyzing power for p^6He scattering. Thus, the negative values of this characteristics contradict to the majority of predictions based on the optical model. And only the special adjustment of the optical potential parameters provides A_y qualitative description.

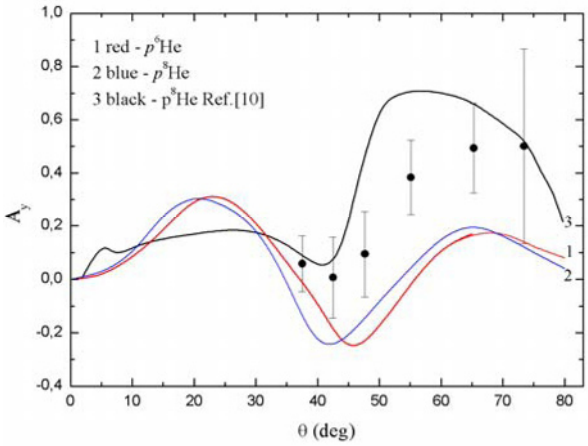

Fig. 2a. The analyzing power of the p^6He (curve 1) and p^8He (curves 2, 3) scattering at $E = 71$ MeV/nucleon. Experimental data are from [3]. Explanations are given in the text.

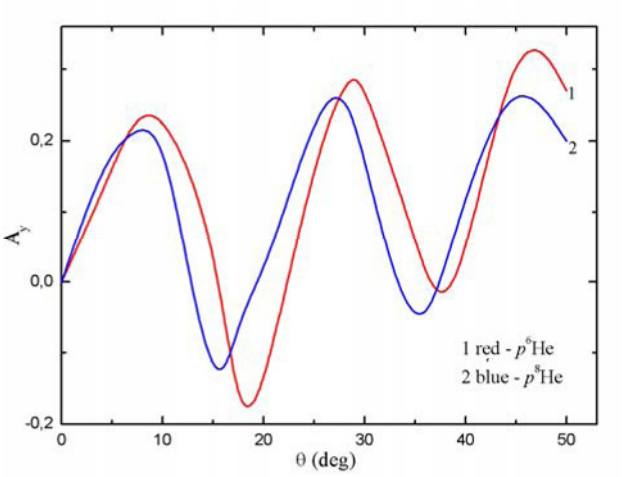

Fig. 2b. The same as in Fig. 2a but at E = 1000 MeV/nucleon.

The upgrade of the RIKEN facility will in principle allow the measurement of the A_y angular distribution for the protons elastic scattering on the He isotopes at somewhat higher energies. Thus we investigated the predictions for the A_y at E = 1000 MeV/nucleon which better correspond to Glauber approach.

Acknowledgments

This work was supported by the Grant Program of the Ministry of Education and Science of the Republic of Kazakhstan 1125/GF.

References

1. T. Uesaka, S. Sakaguchi, Y. Iseri, K. Amos *et al.*, Phys. Rev. C **82**, 021602 (R) (2010)
2. S. Sakaguchi,Y. Iseri, T. Uesaka, M. Tanifuji *et al.*, Phys. Rev C **84**, 024604 (2011)
3. S. Sakaguchi, T. Uesaka, N. Aoi, Y. Ichikawa et al., arXiv : 1302.4237v [nucl-ex] (2013) ; Phys. Rev. C **87**, 021601(R) (2013)
4. I. Tanihata, D. Hirata, T. Kobayachi, S. Shiomura, *et al.*, Phys. Lett. B **289**, 261 (1992)
5. G. D. Alkhasov, M. N. Andronenko, A. V. Dobrovolsky, P. Edelhof *et al.*, Phys. Rev. Let. **78**, 2313 (1997)
6. S. B. Neumaier, G. D. Alkhasov, M. N. Andronenko, A.V. Dobrovolsky *et al.*, Nucl. Phys. A **712**, 247 (2002)
7. O. A. Kiselev, F. Aksouh, A. Bleile, O.V. Bochkarev *et al.*, Eur. Phys. J. A **25**, 215 s01 (2005)
8. A. A. Korsheninnikov, E. Yu. Nikolski, C. A. Bertulani, S. Fukuda e*t al.*, Nucl.Phys. A **617**, 45 (1997)
9. S. Karataglidis, P. Dortmans, K. Amos and C. Bennhold, Phys.Rev. C **61**, 024319 (2000)
10. S. Karataglidis and K. Amos, ArXiv: 1305.1445v [nucl-th], 2013
11. V. I. Kukulin, V. M. Krasnoplski, V. T. Voronchev and P. B. Sazonov, Nucl.Phys. A **453**, 365 (1986)
12. V. I. Kukulin, V. N. Pomerantsev, Kh.D. Razikov *et al.*, Nucl.Phys. A **586**, 151 (1995)
13. E. T. Ibraeva, M. A. Zhusupov, O. Imambekov, and S. K. Sakhiev, Phys. of Part. and Nucl. **42**, 847 (2011)